DOI: 10.13009/EUCASS2017-345

Transonic buffet control by plasma actuator with spark discharge

Andrey A. Sidorenko, Alexey D. Budovsky*, Oleg I. Vishnyakov *, Pavel A. Polivanov* and Anatoly A. Maslov**
**Khristianovich Institute of Theoretical and Applied Mechanics*
Siberian branch of Russian academy of sciences
Institutskaya str. 4/1, Novosibirsk, 630090 RUSSIA

Abstract

The results of experiments on transonic buffet control by means of "plasma wedge" actuators basing on spark discharge are discussed. Experiments have been carried out in the range of Mach number 0.73÷0.78 using model of rectangular wing with supercritical airfoil, chord 200 mm and span 599 mm. Schlieren visualization and Pitot measurements in the wake of the wing show that actuators effectively influence on mean flow and characteristics of shock wave oscillations. It was also found that control efficiency depends on frequency of discharge.

Nomenclature

A	amplitude of shock wave motion [% c]
c	wing chord [mm]
C_x	drag coefficient
F	modulation frequency of discharge [Hz]
f	discharge carrier frequency [Hz]
M	Mach number
P	pressure [Pa]
T	temperature [K]
t	time [s]
x	distance from wing leading edge along wing chord [mm]
y	vertical position perpendicularly freestream direction [mm]
z	spanwise direction [mm]

Greek

α	angle of attack [degree]
γ	adiabatic index
δ	boundary layer thickness [mm]
Δ	difference between measured and reference values

Subscripts

∞	free-stream parameters
0	stagnation parameters

1. Introduction

The problem investigated in the study is very close to the shock waves/turbulent boundary layer interaction (SWBLI) one that poses important theoretical and practical problems that are important for the trans- and supersonic flying vehicles. Fairly strong interactions lead to the appearance of local flow separation regions, which significantly change the pattern of flow and modify the dynamics and heat loads. The phenomenon of turbulent separation in supersonic flows has been extensively studied by experimental methods and numerical simulations [1].

DOI: 10.13009/EUCASS2017-345

The present study is relevant to the problem of shock wave/turbulent boundary layer interaction over the wings at transonic Mach numbers. At transonic speeds the region of supersonic flow arises on the suction side of the airfoil and ended by the strong shock wave. This leads to appearance of additional wave drag of the wing decreasing the aircraft performance in transonic regime. Moreover the interaction of the shock wave with boundary layer produces flow separation and can induces flow instabilities at high angles of attack or Mach numbers. The flow oscillations called "transonic buffet" limit flight Mach number and wing loads reducing the flight efficiency [2, 3]. The wave drag and arising of the flow instability are strongly connected. The problem of transonic buffet is deservedly a matter of scientific and practical interest of large amount of theoretical and experimental studies [4]. One of the pioneer studies concerning unsteady features of the flow over airfoils in transonic flow have been carried out even at the beginning of 50th [5]. But systematical approach to the investigations has been implemented only twenty years later in the experiments with 18% thickness airfoil at zero angle of incidence [6]. Somewhat later, more detailed investigations were performed using a biconvex airfoil with a thickness of 14% [7]. The results of experiments with supercritical airfoils installed at high angles of attack are presented, for example, in the studies [8-12]. One of the urgent scientific challenges in the field still consists in the question concerning the physical mechanisms of the phenomenon, namely the nature of the disturbances and periodical structures embedded intercommunications. It is shown in studies [13, 14] that main mechanism responsible for the buffet onset can be the interaction of the shock with the disturbances generated at airfoil trailing edge or with acoustical one that originate downstream and propagating upstream. At the same time, the pulsation of the separation zone behind the shock wave is the result of the shock wave oscillations and not vice versa. However, analysis presented in [2] showed that the origin of buffet onset is tied to a global instability of the flow. But there are some differences between the mechanisms responsible for the buffet onset on the lifting airfoil at the angle of incidence and symmetrical one at the zero angle of attack even in the similar experimental approach [15].

The practically important efforts in the field are aimed to the development of the flow control techniques capable of decreasing of the wing wave drag and suppressing/delaying buffet oscillations that is highly desirable for increasing of flight efficiency of civil aircraft. One of the well-known passive methods is a cavity under the shock foot covered with a perforated plate [16, 17]. Other passive devices are the grooves and stream-wise slots [18-21]. The main objective of these methods is to weaken the shock and reduce wave drag. But often the wave drag reduction by these techniques is followed by increasing of viscose drag component [22]. The decreasing of the contribution of the viscous drag in the whole one can be achieved by additional control technique such as boundary layer suction through a slot [23, 24]. But this as a rule requires an additional energy consumption. Other passive control method is a bump. 2D bump leads to a significant wave drag reduction, but also results in a high penalties under off-design conditions [25]. More recent studies have been performed with 3D bumps to enhance the off-design performance [26-29].

A lot of different passive and active methods aimed to energize the boundary layer under the shock foot to prevent flow separation were also studied. Vortex generators (VGs) are the most popular method for this purpose. Mechanical VGs were considered in [30-34] and have shown their effectiveness. The main disadvantage of this method is the drag increasing under cruise condition. Air-jet VGs as well as synthetic jet VGs have also been established as effective and very promising for SWBLI control [35-37]. Tangential jet blowing with the same position at 15% to control SWBLI was also investigated in [35]. Further this method was modified and tangential jet was blown near the shock with a relatively small intensity [38-40]. This method was shown is effective for lift increasing. Some of these devices were used in the experiments on buffet control. Mechanical VGs were studied and special mechanical trailing edge device (TED) which can change rear loading of the airfoil was also considered [41]. Fluidic VGs (air-jet VGs) as well as fluidic TED (jet near the trailing edge normal to airfoil pressure side) were studied in [42]. It was shown that mechanical and fluidic VGs were able to delay buffet onset in the angle-of-attack domain by suppressing separation downstream of the shock. The effect of the fluidic TED was different: the separation was not suppressed. In this case, the buffet onset was not delayed in the angle-of-attack domain, but only in the lift domain.

The present study deals with plasma flow control applications, namely, delay of buffet onset on transonic airfoils using plasma discharges. Such kind of the flow control can be potentially advantageous compared to other control techniques. Plasma discharge actuators have simple construction, do not change the aerodynamic shape or influence the wing functionality when they are not in use, allow for smooth variations of forcing frequency and power, and can be used for closed loop feedback control. The results of first experiments in the field of plasma aerodynamics using dielectric barrier discharge (DBD) actuators published in [43]. This type of flow-control devices are well known to introduce not only direct flow acceleration but also periodic disturbances due to periodic flow acceleration in the boundary-layer region, as well as acoustic disturbances [44, 45]. The practical feasibility and efficiency of the plasma discharge technique for subsonic flow control are proved by a lot of experimental investigations [46-48]. The flow control technique has been tested not only in wind tunnel but also in flight experiments [49].

The area concerning the application of electrical discharge to control transonic flow is least investigated nowadays and the results of not numerous studies are not unambiguous. Thus the possibility of shock position control on the

DOI: 10.13009/EUCASS2017-345

profiled plate in transonic flow using dielectric barrier discharge (DBD) was shown in [50]. The direction of control depended on the polarity of DBD electrodes. At the same time, the experiments with DBD used for transonic flow control over NACA3506 airfoil at incidence angle of 8° in the range of Mach number 0.65-0.75 have shown the inefficiency of the discharge actuator [51].
Thus the availability of newly designed control devices is investigated in the study for buffet onset control on the wing with supercritical airfoil. The actuators are based on the interaction of plasma discharge with vertical wedge. Such a configuration provides the formation of longitudinal vortices downstream under asymmetrical energy deposition by plasma discharge as was obtained in preliminary CFD investigations.

2. Experimental Setup

2.1 Wind tunnel and experimental model

The experiments were carried out in TsAGI T-112 transonic wind tunnel with the flow parameters: P_0 = 1 bar, T_0 = 291 K. Free stream Mach number was varied during the experiments. The wind tunnel has a square test section with solid side walls and perforated top and bottom ones (Figure 1). The side walls are equipped by optical windows allowing carrying out schlieren visualization of the flow around the experimental model. The experimental model was the wing of conventional shape with chord length of 200 mm and span 599 mm. The profile of the wing is supercritical airfoil P-184-15SR with max thickness 15% of chord length. The model is equipped by pressure taps distributed at the top and bottom wing surfaces along wing chord. The experimental model has been made from steel and has a cavity on the upper surface for plasma actuator insert installation (Figure 1). Boundary layer transition was triggered at 15% of chord length on both surfaces of the wing. The flow around the model was studied by schlieren visualization, surface pressure distribution measurements and Pitot measurements in the wake of the wing using Pitot rake located vertically in the middle section downstream of the model (see Figure 1b). The 48-channel unit based on strain-gage pressure sensors with the range of 100 kPa was used for Pitot measurements in the wake. The reduced error of pressure measurements of the unit not more than 0.15% for each channel.

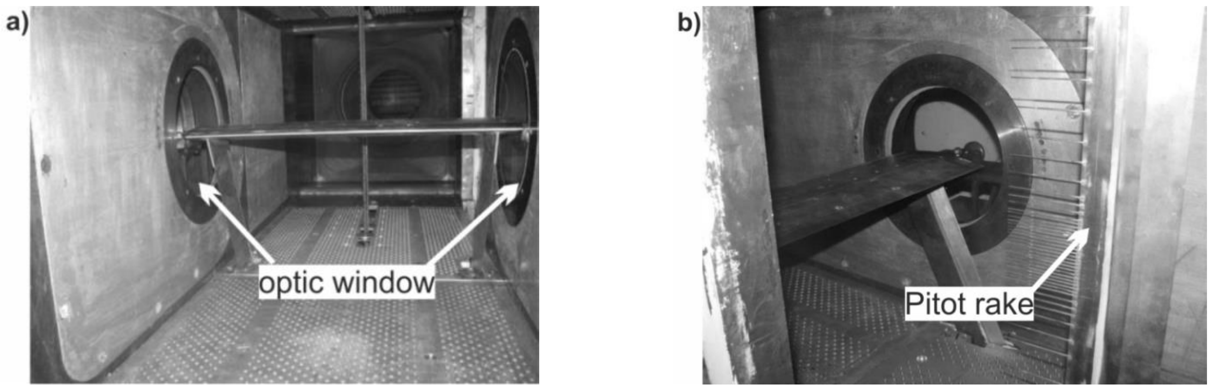

Figure 1: Photos of the experimental model in T-112 test section; view from leading (a) and trailing (b) edge

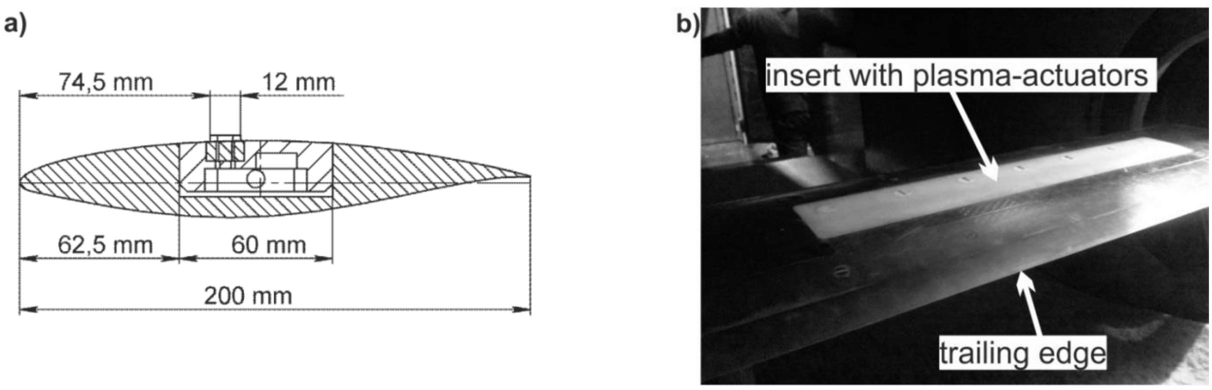

Figure 1: Draft (a) and photo (b) of the experimental model equipped with plasma actuator insert

DOI: 10.13009/EUCASS2017-345

2.2 Plasma actuators and high-voltage equipment

The flow control strategy accepted in the study was intensification of the momentum exchange in the boundary layer upstream on the shock wave boundary layer interaction region. An intensive preliminary CFD study revealed that steady surface energy deposition may lead only to decrease of momentum in the boundary layer. It means that such actuator may effectively provoke the flow separation but is unable to delay it. For delaying or suppressing of the flow separation downstream of the shock the combined actuator was found to be the most efficient. This actuator consists of vertical wedge aligned with local streamlines and protruding in the flow by 0.4-0.8·δ. In passive state it has minimum effect on the flow (Figure 2a, Figure 3a). If plasma is initiated on one side of the wedge it results in increasing of streamwise vorticity downstream. Distribution of wall shear stress near the actuator and in the wake under energy deposition is shown in Figure 2b. In this case, the volume energy source is placed on the left side of the wedge (bottom side in the figure). Figure 3b shows distribution of mass flow in the cross section downstream of the actuator. It can be seen from the figures that asymmetrical energy deposition leads to formation of longitudinal vortex downstream of the actuator (Figure 2b) and intensification of momentum exchange in the boundary layer (Figure 3b).

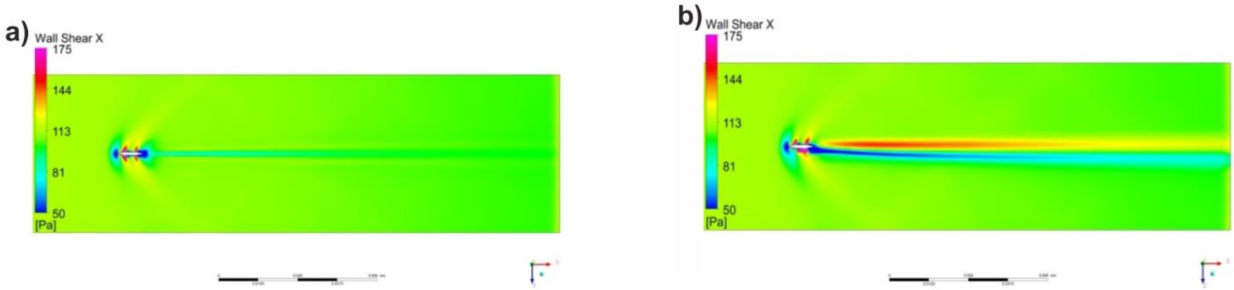

Figure 2: Wall shear stress for the plasma off case (a) and excited actuator (b)

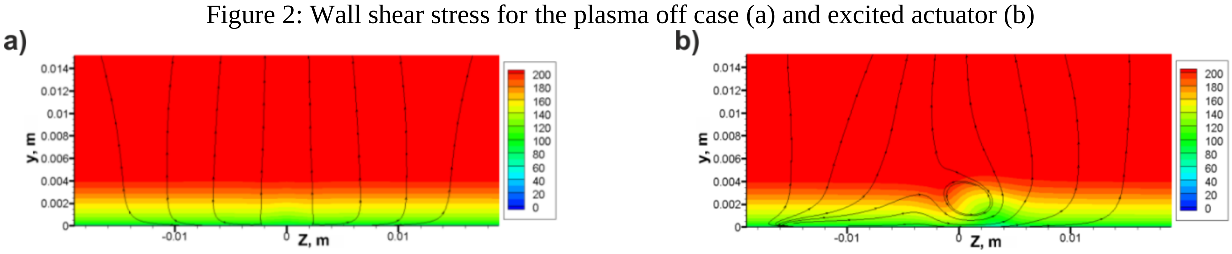

Figure 3: Distribution of mass flow and streamlines in the wake for the plasma off case (a) and excited actuator (b)

Basing on the data obtained in CFD the “plasma-wedge” actuator was designed and manufactured. The actuator consists of dielectric body made from machinable glass-ceramic MACOR and pair of cooper electrodes. The actuator insert used in wind tunnel experiments has been equipped by several “plasma wedge” actuators distributed along the span (Figure 4). The leading and trailing edge of the wedge are located at the 74.5 mm and 86.5 mm respectively (37%, 43% of chord) from leading edge of the wing (see Figure 1a). The total number of wedge actuators is 5, the spanwise distance between the elements is 60 mm. The height of the wedge is 1.3 mm, the length is 12 mm and thickness (span) is 1 mm. The electrodes for spark discharge are flush mounted on the insert surface close to the wedge at the one side so as the length of discharge gap is 6 mm (upstream and downstream electrodes are located at 77.5 mm and 83.5 mm respectively from the leading edge of the wing).

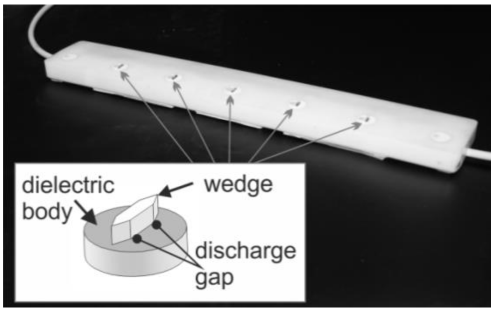

Figure 4: Photo of “plasma-wedge” actuator insert and 3D model of the actuator

To excite the “plasma-wedge” actuators the multichannel short duration pulse high-voltage generator (HVG) was used (Figure 5). The HVG consists of: pulse driver based on thyratron Th, 6ηF capacitors C1 and C2, saturable

DOI: 10.13009/EUCASS2017-345

inductors L1 and L2, pulse charging unit with untransformed power supply scheme, trigger unit that control the pulse repetition frequency and allowing synchronization of pulse driver, charging unit C3 and other external devices. The pulse driver output is connected with discharge gap by 1.5m coaxial wire. The capacity of the wire (100ρF/m) serves simultaneously as intensifying capacity that allows increasing of current amplitude after electrical breakdown at discharge gap. Thus the voltage potential in node *1* turns into reverse polarity after thyratron opening. As a result the negative pulse of doubled amplitude is formed in node *2* having a front of about 250ηs. This pulse with time delay of 200ηs saturates the inductor L2 and thus forms the negative pulse in node *3* with front duration of 100ηs. The amplitude of output voltage can be varied before the electrical breakdown in the range from 10 kV up to 30kV. The HVG provides the following excitation parameters: pulse amplitude ≤ 30kV, pulse rise time ≤ 200 ηs, pulse energy ~2 J, excitation frequency up to 3.5 kHz, duration of energy deposition (after discharge breakdown) ≤ 2 μs, average power using matched load is equal to 1 kW.

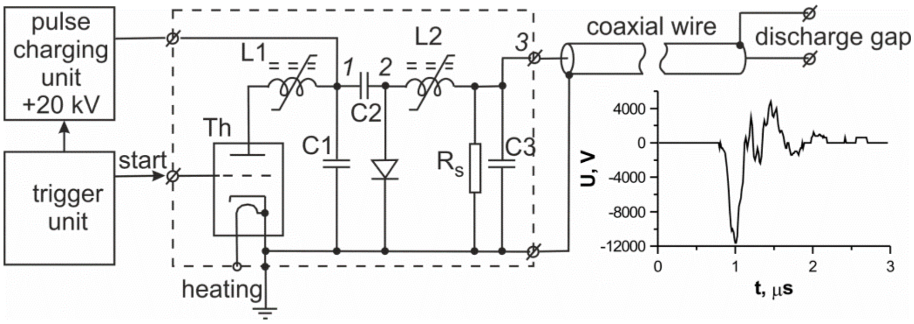

Figure 5: Electrical circuit of HVG and voltage form at output

The HVG can operate in continuous and modulated mode. In the latter case the high voltage signal with driving frequency *f* is gated by the lower frequency *F* using external generator. The average power of the discharge in this case does not depend on the frequency *F* if the duty cycle is constant. In the present experiments the modulation frequency *F* was varied in the range 50÷100 Hz while the carrier one was fixed and equal to *f* = 1500Hz. The duty cycle of the modulation was 0.5.

The discharge parameters in the experiments were measured by means of two-channel 100 MHz ADS-2111MV AKTAKOM oscilloscope, 75 MHz Tektronix P6015A high voltage probe, 60 MHz Tektronix P6021 current probe. The discharge parameters measured in the experiments for excitation frequency *f* = 1.5 kHz are follow: pulse amplitude ~12kV, pulse rise time ~ 200 ηs, pulse energy ~0.12 J, electric power ~180 W (6 kW/m).

3. Data processing techniques

Due to high risk of damage of any pressure sensors by electrical noise generated by discharge the only technique that is able to provide the unsteady parameters of the flow in present experiments was schlieren visualization. The visualization was performed using high speed camera Motion Xtra N3. The frame rate frequency was 5 kHz in present experiments. The analysis of schlieren pictures is quite complicated due to 3D structure of the flow. An example of the visualization and results of corresponding data processing are presented in Figure 6. The original flow structure in the interaction region is shown in Figure 6a. Figure 6b and Figure 6c present the results of automatic image recognition by two different image processing methods.

The image recognition technique is aimed for detection of shock wave (SW) position in each frame of schlieren video data to derive the amplitude and frequency of the shock wave oscillation. The image recognition was performed by several algorithms.

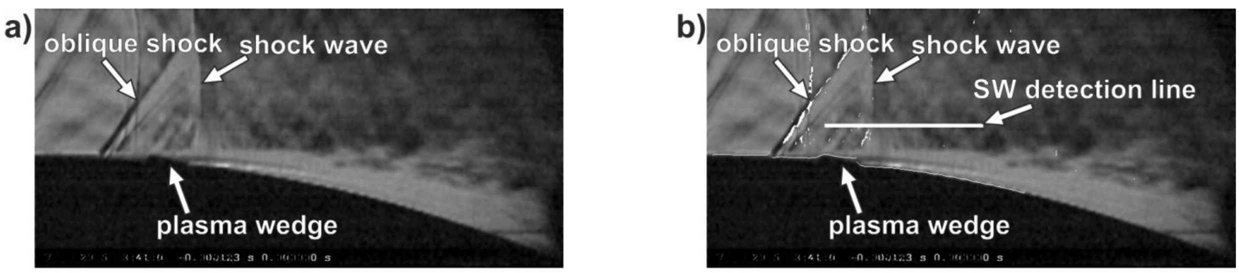

DOI: 10.13009/EUCASS2017-345

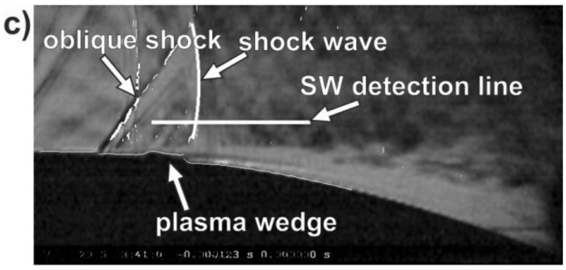

Figure 6: Example of instantaneous schlieren visualization (a) and results of data processing by method #1 (b) and method #2 (c)

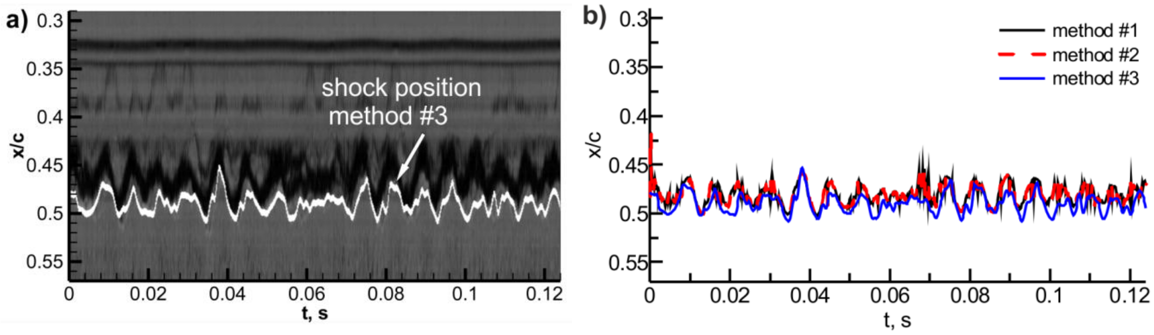

Figure 7: Distribution of schlieren image intensity *vs* time with SW position line obtained by method 3 (a) and comparison of different detection algorithm (b) (M_∞=0.76, α = 5°)

The first algorithm recognizes the shock wave as a region of maximum streamwise intensity gradient. The regions can be seen in Figure 6b and Figure 6c as the white fields. As there are additional regions of high gradient in the frames and the shock is curved its position was sought along the definite line at a distance of about 10 mm from wing surface (white horizontal line in the figures). It can be seen for example from Figure 6b that this technique is not able to detect the whole front of the shock wave. Therefore the algorithm produces some sporadic errors.

The second method was developed to increase reliability of the results of shock wave detection. In this case a pattern of SW front is manually defined as a curved line (see Figure 6c) once for the first frame and the algorithm searches its position in the each following frame of schlieren data set by correlation technique. The position of SW was also defined at a distance of 10 mm from wing surface.

The third method takes into account only streamwise distribution of the image intensity at a distance 10 mm from the surface for each frame. In this case the data are analyzed as time-bases of image intensity at this distance as shown in Figure 7a. The shock oscillation can be seen from the figure as white border between light and dark regions. This line is detected by gradient technique providing the time history of shock wave motion.

The oscillograms of shock wave oscillations revealed by these three techniques are shown in Figure 7b. The vertical axis corresponds to the distance from wing leading edge and the horizontal one corresponds to the record time of corresponding frame. In the most of tests this period was rather short (103 ms) due to limitation of the recording equipment.

4. Experimental results

The experiments were carried out for M_∞ = 0.73, 0.74, 0.76, 0.78 at the angle of attack of the wing α = 5° corresponding to beginning of buffet regime for this particular airfoil. The discharge frequency and excitation mode were varied. For each experiment the following data were obtained: high-speed schlieren visualization and vertical distribution of Pitot pressure measured in the wake downstream of the model using pressure rake.

4.1 Study of discharge frequency effect

The data on discharge frequency and excitation regime were obtained for fixed flow parameters M_∞ = 0.76 and α = 5°. This combination of M_∞ and α corresponds to the beginning of the buffet onset as was obtained in the preliminary study with clear wing without discharge actuators. Figure 8 and Figure 9 show Pitot pressure distributions in the wake of the model. Note that the rake was placed in the center of test section. The vertical axis in

DOI: 10.13009/EUCASS2017-345

the figures is pressure difference between measured Pitot pressure and P_0. The horizontal axis is y position of the sensor in the rake.

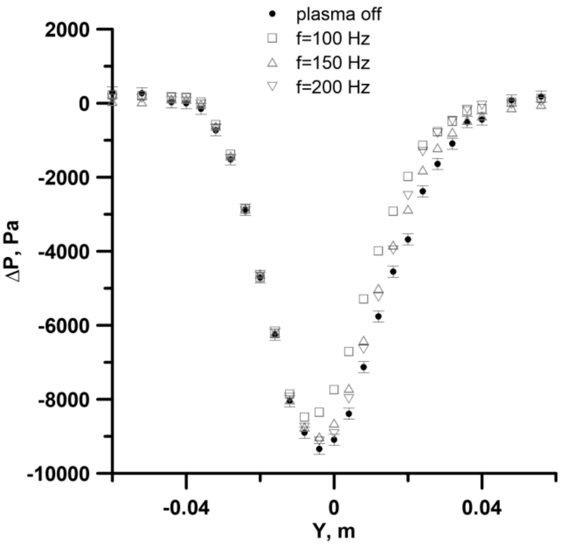

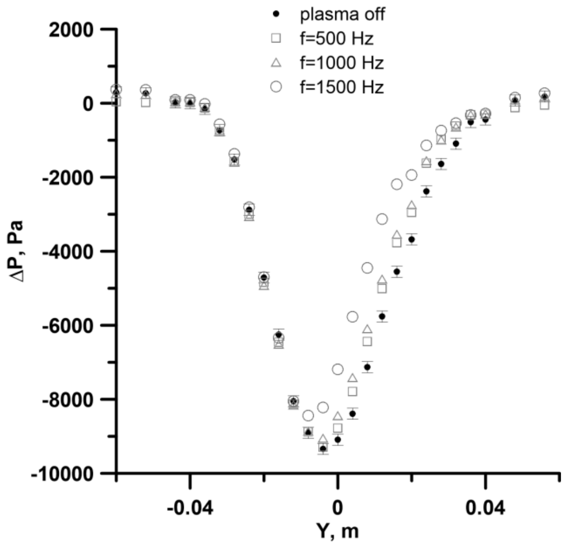

Figure 8: Pitot pressure distribution in the wake for continuous mode of discharge excitation (M_∞=0.76, α = 5°)

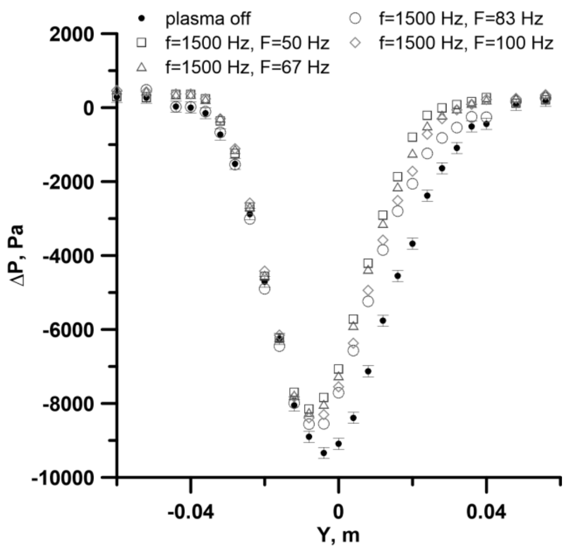

Figure 9: Pitot pressure distribution in the wake for modulated mode of discharge excitation (M_∞=0.76, α = 5°)

Analysis of these data reveals that wake pressure distribution changes due to plasma excitation near the wedge. There is evident change of the wake width and pressure magnitude for the cases of energy deposition in comparison with reference one. The strong effect is observed for the low frequency f = 100 Hz at continuous mode of plasma excitation (see Figure 8a). This frequency is about 30-40 Hz lower than buffet frequency measured in the experiments. The data show that the wake becomes narrow. This can be connected with suppression of flow separation on the leeward surface of the wing due to plasma excitation while the shear layer caused by bottom part of the wing remains the same for all variants of energy deposition. It is interesting to note that increasing of the discharge frequency up to 1000 Hz results in recovery of the wake to the reference state. The effect of plasma decreases while the average discharge power is increased with increasing of excitation frequency. But increasing of excitation frequency up to 1500 Hz lead again to almost the same converging of the wake as it was obtained for f = 100 Hz (Figure 8b). It means that the mechanism of plasma flow control is connected with unsteady processes in the separation zone and control efficiency depends on frequency of energy deposition.

The data obtained in modulated regime of discharge excitation are presented in Figure 9. It is seen from the figure that in all of test cases the width of the wake significantly decreases due to discharge excitation in comparison with the reference case. The strongest effect is observed for F = 50 Hz.

DOI: 10.13009/EUCASS2017-345

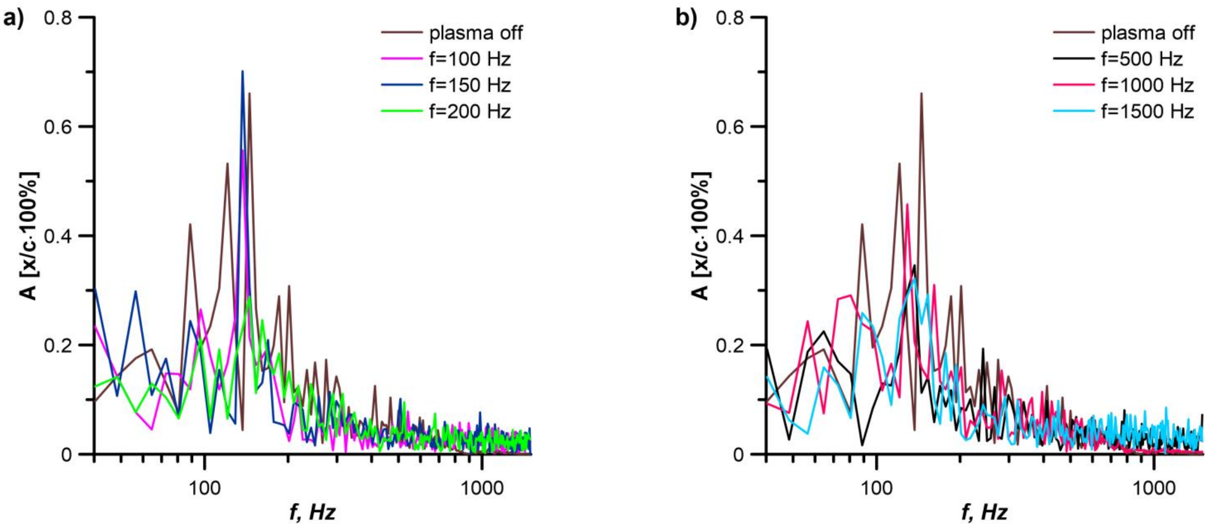

Figure 10: Spectra of SW motion at continuous mode of discharge excitation (M_∞=0.76, α = 5°)

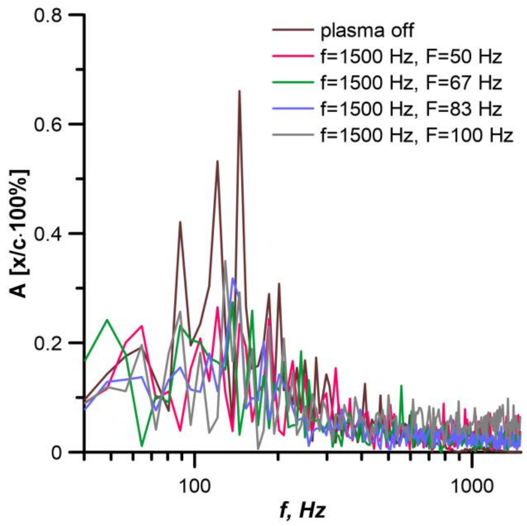

Figure 11: Spectra of SW motion at continuous mode of discharge excitation (M_∞=0.76, α = 5°).

The spectra of SW oscillations obtained basing on the results of schlieren data processing as described above are shown in Figure 10 and Figure 11. In spite of short time of data acquisition it is possible to reveal the main characteristics of unsteady processes. It can be seen that for the reference case the main peak corresponds to the buffet frequency of 135÷140 Hz. There are also additional peaks at frequencies about 80 and 110 Hz. Excitation of plasma in continuous mode (Figure 10a, b) results in stabilization of SW oscillations. It can be seen from the figures that amplitudes of the main and other peaks significantly decrease if the plasma actuators are excited and the strongest effect is achieved at excitation frequency 200 and 1500 Hz. There is only one case where the amplitude of the main peak increases (f = 150 Hz) corresponding to the discharge frequency matched to buffet one. However in this case the amplitude of the other peaks also significantly decreases. It is seen from Figure 11 that plasma excitation in modulated mode also lead to decreasing of shock oscillations intensity.
Comparison of the data presented reveals the fact that the unsteady behavior of the shock wave and flow pattern in the wake are connected. Intensive oscillations of the shock and separation region result in higher level of pressure losses measured downstream of the wing.

4.2 Study of Mach number effect

The study of Mach number effect has been carried out at fixed value of the angle of attack of the wing α = 5° while the Mach number was varied in these experiments. Time-bases of schlieren images intensity obtained for α = 5° and M = 0.73, 0.74, 0.76 and 0.78 (along the line at distance about 10mm from wing upper surface) are presented in Figure 12. For each value of Mach number three test cases were considered: reference case without discharge,

DOI: 10.13009/EUCASS2017-345

continuous mode of discharge excitation at carrier frequency 1500 Hz (about an order higher of buffet frequency) and discharge excited in modulated regime (f = 1500 Hz, F = 100 Hz). At pre-buffet conditions (M = 0.73, α = 5°) the nonharmonic SW oscillations with low amplitude are observed.The continuous discharge excitation almost eliminates these oscillations. Plasma excitation in modulated mode seems does not provide any effect. In the next test case for M = 0.74 the shock wave oscillations are well recognized. This combination of M and α corresponds to the beginning of buffet onset. It is clearly seen from the corresponding figures that in this case continuous discharge excitation result in the buffet suppression while the modulated excitation is not so effective. Increasing of Mach number up to 0.76 results in evident buffet onset with well seen harmonic oscillations of the shock wave. Here the plasma excited in continuous mode also suppresses the oscillations but not completely eliminates them. In the test case of M_∞ = 0.78 the analysis of the intensity time-bases is complicated due to additional shocks presenting in the frame. Therefore the effect of discharge excitation is not obvious in this case.

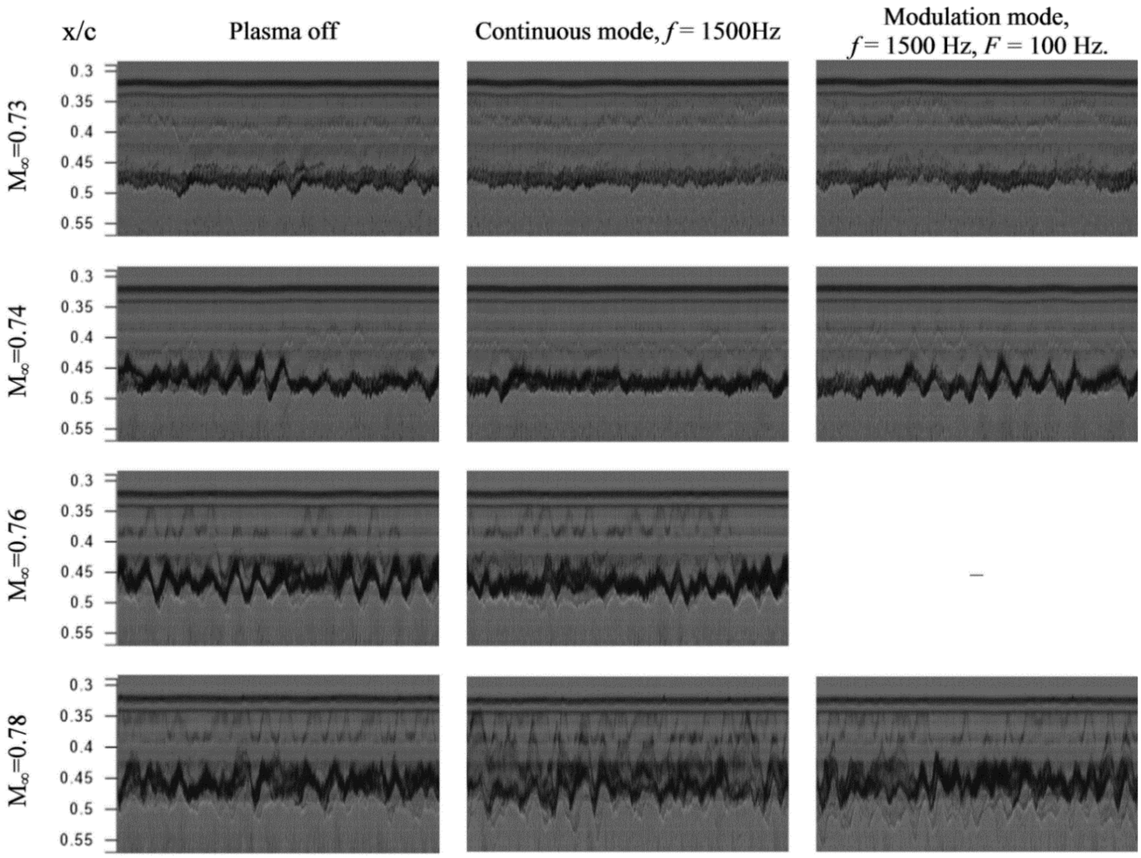

Figure 12: Intensity distribution along chord *vs* time for α = 5° and various Mach numbers

Pressure distributions in the wake reveal the strongest effect for the test case of M_∞ = 0.74 and M_∞=0.76 (Figure 13b,c). In both cases excitation of plasma result in increasing of pressure losses in the wake. Note that data presented for the test case of M_∞=0.76, α=5° are in certain contradiction with the data shown in Figure 8, Figure 9 where the width of the wake was decreased under continuous energy deposition at f = 1500 Hz. Here we have the opposite effect.
The corresponding spectra are shown in Figure 14. For the test case of M = 0.73 there are just very small peaks corresponding to the shock wave oscillations. The discharge excitation does not influence on the oscillation frequency however it can be seen that low frequency oscillations are considerably dumped at continuous mode of discharge excitation. For the case of M = 0.74 the peak of shock wave oscillation corresponding to f = 150 Hz are easy to see on the spectrum for reference case. This peak is completely dumped by the discharge excited in continuous mode but in the case of modulated mode of discharge excitation the amplitude of this peak increased in twice. The same result can be observed for the case of M = 0.76 where the shock wave oscillations were significantly decreased by plasma excited in continuous mode. The oscillations of the shock for the case of M = 0.78 are more

DOI: 10.13009/EUCASS2017-345

intense with several peaks in the spectrum. It can be seen from the figure that excitation of discharge in both continuous and modulated regimes leads to significant increasing of low frequency oscillations.

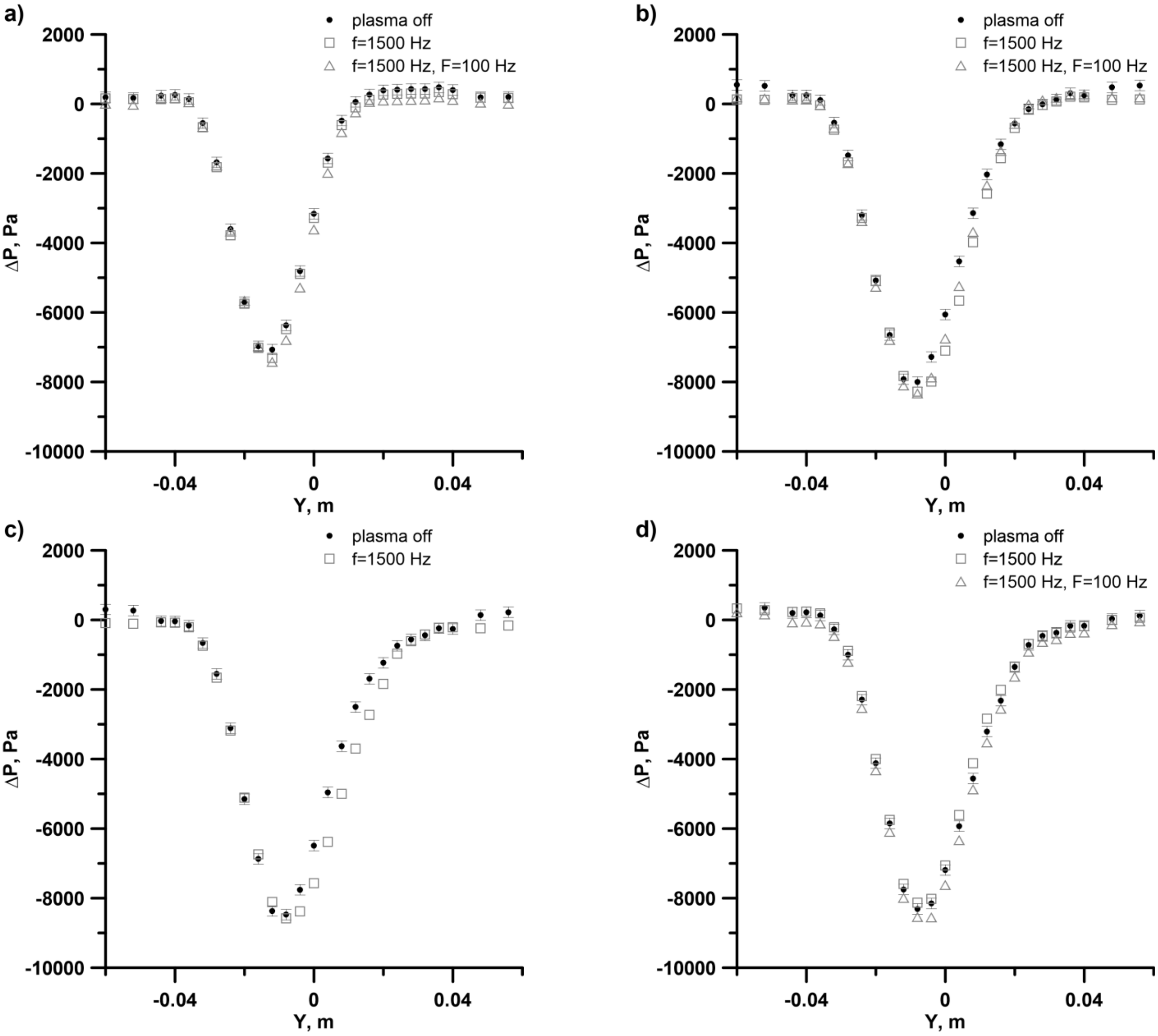

Figure 13: Pressure distribution in the wake at α=5° for M=0.73(a), M=0.74(b), M=0.76(c) and M=0.78(d)

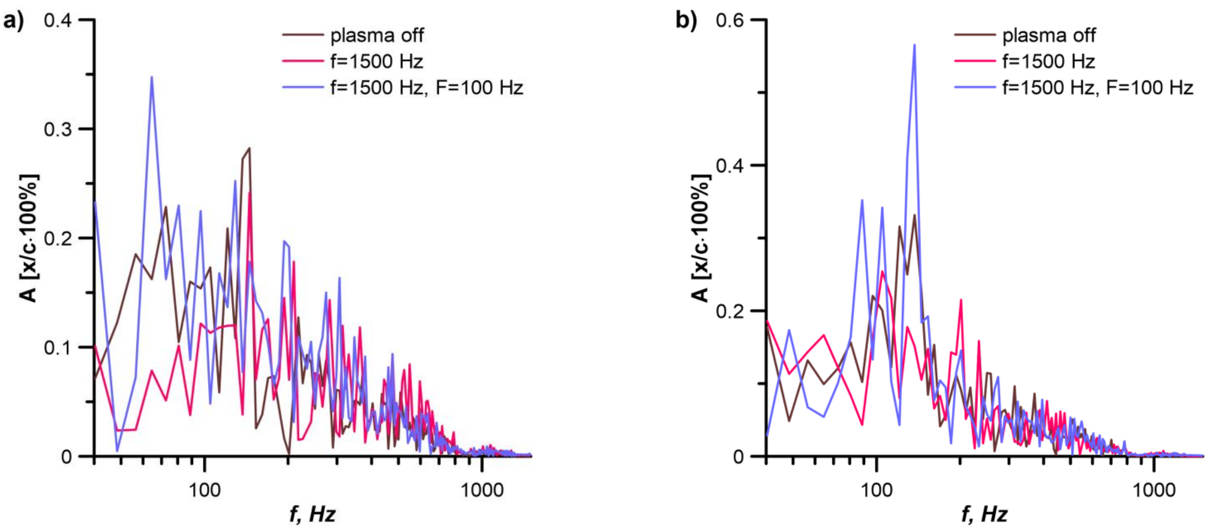

DOI: 10.13009/EUCASS2017-345

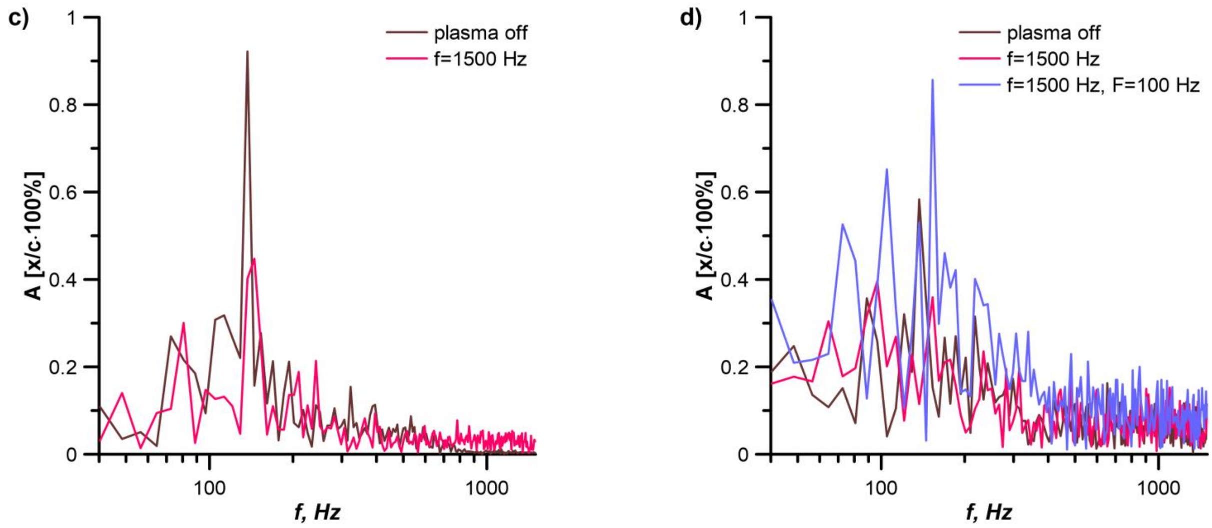

Figure 14: Spectra of shock wave oscillation at α=5° for M=0.73 (a), M=0.74 (b), M=0.76 (c) and M=0.78 (d)

The integral influence of plasma actuators on buffet as well as aerodynamic characteristics of the wing model can be seen from Figure 15. The data on standard deviations (std) of shock wave position depending on Mach number are presented in Figure 15a. The deviations have been calculated as integral of corresponding power spectra of shock wave pulsations in the frequency range 80 ÷ 220 Hz that contain the frequency of buffet. The influence of the actuators on drag coefficient of the model is shown in Figure 15b. The drag coefficient has been calculated basing on the data on pressure losses measured by pressure rake in the wake of the model using the following equation:

$$C_x = 2 \cdot \int_{\bar{y}_1}^{\bar{y}_2} \left\{ \sqrt{ \frac{ \left[\frac{p(\bar{y}) + p_0}{p_\infty}\right]^{\frac{\gamma-1}{\gamma}} - 1 }{ \left[\frac{p_0}{p_\infty}\right]^{\frac{\gamma-1}{\gamma}} - 1 } \cdot \left(\frac{p(\bar{y}) + p_0}{p_0}\right)^{\frac{\gamma-1}{\gamma}} } - \left(\frac{ \left[\frac{p(\bar{y}) + p_0}{p_\infty}\right]^{\frac{\gamma-1}{\gamma}} - 1 }{ \left[\frac{p_0}{p_\infty}\right]^{\frac{\gamma-1}{\gamma}} - 1 } \right) \right\} dy$$

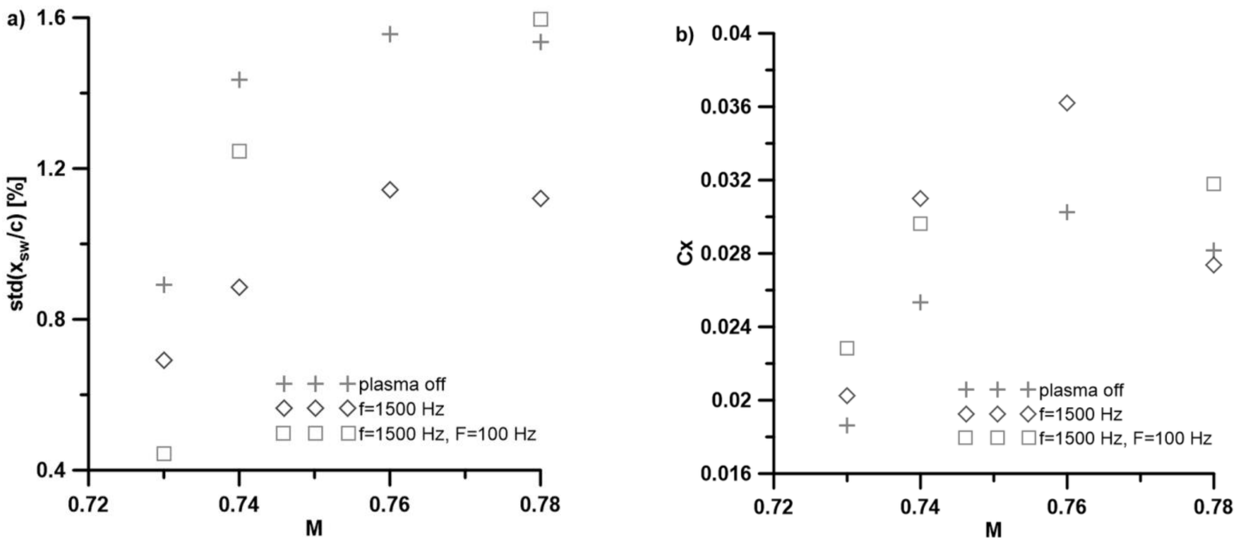

Figure 15: Standard deviation of shock wave pulsation (a) and drag coefficient depending on Mach number (b) at α=5°

It is seen from the figures that increasing of Mach number up to 0.76 is followed by intensification of shock wave pulsations (Figure 15a) as well as leads to increasing of drag (Figure 15b) caused by increasing of pressure losses in the wake of the model. Using of plasma wedge actuators results in dumping of shock wave pulsations but followed by increasing of drag in comparison with reference case. It is seen that in the range of Mach numbers 0.73-0.76 the effect of plasma wedge actuator is conceptually the same both for continuous and modulated regime of discharge excitation but is most pronounced for the first one. At Mach number 0.78 it is seen that actuators excited in modulated mode lead to intensification of shock wave oscillations and drag increasing while continuous mode of excitation demonstrate the opposite effect.

4. Conclusions

The study concerning plasma discharge actuators influence on transonic flow namely buffet suppression/delay has been performed in the range of Mach numbers using model of rectangular wing at incidence angle of 5°. The flow control was implemented by means of “plasma wedge” actuators that are based on spark discharge. The parameters of discharge such as excitation frequency and excitation mode (continuous/modulated) were varied in the experiments.

Comparison of the data obtained reveals the fact that the unsteady behavior of the shock wave and flow pattern in the wake are connected. Intensive oscillations of the shock and separation region are followed by higher level of pressure losses measured downstream of the wing.

The data obtained experimentally show that “plasma-wedge” actuators can be considered as effective devices to control the oscillations of the shock wave. The results show that the actuator is able to influence on the mean flow and flow pulsations characteristics. Thus excitation of plasma wedge actuators results in dumping of shock wave pulsations but is followed by increasing of drag in comparison with reference case with unexcited actuator. It is also obtained that at certain conditions the excitation of actuators can provide both buffet suppression and drag decreasing together. The data analysis shows that there is a selective receptivity of the flow to discharge excitation frequency as the increasing of the frequency does not guarantee the increasing of the control efficiency.

Acknowledgments

This work was supported by BUTERFLI Project of the 7th Framework Program of the European Commission (Grant Agreement 605605), grant of Russian Foundation for Basic Research 16-08-01134A and grant of Russian Scientific Foundation No. 16-19-10407 (TsAGI, data post-processing).

References

[1] Dolling DS. 2000. 50 Years of Shock Wave/Boundary Layer Interaction Research—What Next? *AIAA Paper 2000-2596.*

[2] Crouch JD, Garbaruk A, Magidov D and Travin A. 2009. Origin of transonic buffet on aerofoils. *J. Fluid Mech doi:10.1017/S0022112009006673*

[3] Molton P, Dandois J, Lepage A, Brunet V and Bur R. 2013. Control of Buffet Phenomenon on a Transonic Swept Wing. *AIAA J. 51(4):761-772.*

[4] Szumowski AP, Meier GEA. 1996. Forced oscillations of airfoil flows. *Exp. Fluids 21:457 – 464.*

[5] Humphreys MD. 1951. Pressure pulsations on rigid airfoils at transonic speeds. *NACA RM L51I12, National Advisory Committee for Aeronautics.*

[6] McDevitt JB, Levy Jr LL, Deiwert GS. 1976. Transonic flow past a thick circular-arc airfoil. *AIAA J. 14(5):606 – 613.*

[7] Mabey DG, Welsh BL, Cripps BE. 1981. Periodic flows on a rigid 14% thick biconvex wing at transonic speeds. *TR 81059, Royal Aircraft Establishment*

[8] Roos FW. 1975. Surface pressure and wake flow fluctuations in a supercritical airfoil flow field. *AIAA Paper 75-66*

[9] Hirose N, Miwa H. 1988. Computational and experimental research on buffet phenomena of transonic airfoils. *NAL Report TR-996 T, National Aerospace Laboratory, Japan*

[10] Lee BHK (1989) Investigation of flow separation on a supercritical airfoil. J. Aircraft 26(11):1032-1037

[11] Lee BHK. 1991. An experimental investigation of transonic flow separation. *In Zhuang FG(ed) Recent Advances Experimental fluid mechanics, Proceedings of First International Conference on Experimental Fluid Mechanics, Chengdu, China. Int. Academic Publishers, Beijing, China. pp 199-204*

[12] Stanewsky E, Basler D. 1990. Experimental investigation of buffet onset and penetration on a supercritical airfoil at transonic speeds. *AGARD CP-483, Aircraft dynamic loads due to flow separation, Sorrento, Italy. pp4.1-11*

DOI: 10.13009/EUCASS2017-345

[13] Lee BHK. 2001. Self-sustained shock oscillations on airfoils at transonic speeds. *Progress in Aerospace Science 37:47-196*
[14] Hartmann A, Klaas M, Schröder W. 2012. Time-resolved stereo PIV measurements of shock–boundary layer interaction on a supercritical airfoil. *Exp Fluids. doi:10.1007/s00348-011-1074-6*
[15] Zijie Zhao Xudong Ren, Chao Gao. 2013. Experimental Study of Shock Wave Oscillation on SC(2)-0714 Airfoil. *AIAA Paper 2013-0537*
[16] Bahi L, Ross JM, and Nagamatsu T. 1983. Passive shock wave/boundary layer control for transonic airfoil drag reduction. *AIAA Paper 1983-0137*
[17] Bur R, Corbel B and Délery J. 1998. Study of Passive Control in a Transonic Shock Wave/Boundary Layer Interaction. *AIAA Journal, 36(3):394-400*
[18] Raghunathan S. 1988. Passive control of shock-boundary layer interaction. *Progress in Aerospace Science, 25:271-296*
[19] Smith AN, Holden HA, Babinsky H, Fulker JL and Ashill PR. 2003. Normal Shock-Wave/Turbulent Boundary Layer Interactions in the Presence of Streamwise Slots and Grooves. *Aeronautical Journal. 106:493-500*
[20] Holden HA and Babinsky H. 2005. Separated Shock-Boundary-Layer Interaction Control Using Streamwise Slots. *Journal of Aircraft 42(1):166-17*
[21] Babinsky H and Ogawa H. 2006. Three-Dimensional SBLI Control for Transonic Airfoils. *AIAA Paper 2006-3698*
[22] Stanewsky E, Délery J, Fulker JL and Geissler W. 1997. Synopsis of the Project EUROSHOCK. Notes on Numerical Fluid Mechanics: Drag Reduction by Passive Shock Control. *Results of the Project EUROSHOCK, Vol. 56, Vieweg Ed., Wiesbaden (Germany). pp1-81*
[23] Délery J, Bur R. 2000. The Physics of Shock Wave / Boundary Layer Interaction Control: Last Lessons Learned. *Proceedings of the ECCOMAS 2000 Congress, Barcelona (Spain). pp11-14*
[24] Stanewsky E, Délery J, Fulker JL and De Matteis P. 2002. Synopsis of the Project EUROSHOCK II. Notes on Numerical Fluid Mechanics and Multidisciplinary Design: Drag Reduction by Shock and Boundary Layer Control - *Results of the Project EUROSHOCK II, Vol. 80, Springer Ed., Berlin (Germany). pp.1-124*
[25] Birkemeyer J, Rosemann H and Stanewsky E. 2000. Shock Control on a Swept Wing. *Aerospace Science and Technology 4:147-156*
[26] Lin JC. 1991. Exploratory Study of Vortex-generating Devices for Turbulent Flow Separation Control. *AIAA Paper 91-0042*
[27] Wong WS, Qin N, Sellars N, Holden HA and Babinsky H. 2008. A Combined Experimental and Numerical Study of Flow Structures over Three-Dimensional Shock Control Bumps. *Aerospace Science and Technology. 2:436-447*
[28] Ogawa H, Babinsky H, Pätzold M and Lutz T. 2008. Shock-Wave/Boundary-Layer Interaction Control Using Three-Dimensional Bumps for Transonic Wings. *AIAA Journal. 46(6):1442-1452*
[29] Colliss SP, Babinsky H, Bruce PJK, Nübler K and Lutz T. 2012. An Experimental Investigation of Three-Dimensional Shock Control Bumps Applied to Transonic Airfoils. *AIAA Paper 2012-0043*
[30] Gadetskiy VM, Serebriyskiy YaM, and Fomin VM. 1974. Investigation of the influence of vortex generators on turbulent boundary layer separation. *NASA TT F-16056.*
[31] Mounts JS and Barber TJ. 1992. Numerical Analysis of Shock-Induced Separation Alleviation Using Vortex Generators. *AIAA Paper 92-0751*
[32] McCormick DC. 1993. Shock-Boundary Layer Interaction with Low Profile Vortex Generators and Passive Cavity. *AIAA Journal. 31(1):96*
[33] Godard G and Stanislas M. 2006. Control of a Decelerating Boundary Layer. Part 1: Optimization of Passive Vortex Generators. *Aerospace Science and Technology 10:181-191*
[34] Holden HA and Babinsky H. 2007. Effect of Microvortex Generators on Separated Normal Shock / Boundary Layer Interactions. *Journal of Aircraft. 44(1):170-174*
[35] Pearcey HH. 1961. Shock-induced separation and it's prevention by design and boundary layer control, In: Boundary layer and flow control – it's principles and application. Ed. by Lachmann. *Vol. 2. London. Pergamon Press, pp1170-1361*
[36] Rao MK. 1988. An Experimental Investigation of the Use of Air Jet Vortex Generators to Control Shock Induced Boundary Layer Separation. *PhD Dissertation, City University*
[37] Pearcey HH, Rao K, and Sykes DM. 1993. Inclined Air-Jets Used as Vortex Generators to Suppress Shock-Induced Separation. *Paper No. 40 in AGARD CP-534, Fluid Dynamics Panel Symposium on Computational and Experimental Assessment of Jets in Crossflow, Winchester, UK*
[38] Bokser VD, Wolkov AV, and Petrov AV. 2009. Application of tangential jet blowing for reduction of drag for supercritical airfoils at high subsonic speeds. *TsAGI Science Journal, 40(1):9–21*
[39] Petrov AV, Bokser VD, Sudakov GG and Savin PV. 2010. Application of tangential jet blowing for suppression of shock-induced flow separation at transonic speeds. *ICAS Paper 2010-3.7.2*

[40] Petrov AV. 2011. Energy methods of increase of wing lift. *Fizmatlit, Moscow.*
[41] Caruana D, Mignosi A, Robitaille C and Correge M. 2003. Separated Flow and Buffeting Control. *Flow, Turbulence and Combustion, 71:221-245.*
[42] Dandois J, Molton P, Lepage A, Geeraert A, Brunet V, Dor, J-B and Coustols E. 2013. Buffet Characterization and Control for Turbulent Wings. *Aerospace Lab Journal. http://www.aerospacelab-journal.org/al6/buffet-characterization-and-control-for-turbulent-wings.*
[43] Roth JR, Sherman DM and Wilkinson SP. 1998. Boundary layer flow control with a one atmosphere uniform glow discharge surface plasma. *AIAA Paper 98-0328, AIAA 36th aerospace sciences meeting and exhibit, Reno, NV. DOI:10.2514/6.1998-328*
[44] Roth JR, Xin Dai. 2006. Optimization of the aerodynamic plasma actuator as an electrohydrodynamic (EHD) electrical device. *AIAA 2006-1203, AIAA 44th aerospace sciences meeting and exhibit, Reno, NV. DOI:10.2514/6.2006-1203*
[45] Baird C, Enloe CL, McLaughlin TE and Baughn JW. 2005. Acoustic testing of the dielectric barrier discharge (DBD) plasma actuator. *AIAA 2005-565, AIAA 43rd aerospace sciences meeting and exhibit, Reno, NV. doi:10.2514/6.2005-565*
[46] Moreau E. 2007. Airflow control by non-thermal plasma actuators. *J. Phys. D: Appl. Phys. 40 605. DOI:10.1088/0022-3727/40/3/S01*
[47] Malmuth ND, Maslov AA, Sidorenko AA, Fomichev VP, Korotaeva TA. 2008. ITAM Study of Aerodynamics in Weakly Ionized Plasma. *AIAA Paper 2008-4336. DOI: 10.2514/6.2008-4336*
[48] Corke TC, Enloe CL and Wilkinson SP. 2010. Dielectric Barrier Discharge Plasma Actuators for Flow Control. *Annual Rev. of Fluid Mech. Vol. 42. p. 505-529.*
[49] Sidorenko AA, Budovsky AD, Pushkarev A, Maslov AA. 2008. Flight Testing of DBD Plasma Separation Control System. *AIAA Paper 2008-373. AIAA 46th aerospace sciences meeting and exhibit, Reno, NV. DOI: 10.2514/6.2008-373.*
[50] Yuriev AS, Korzh SK, Pirogov SYu, Savischenko NP, Leonov SB, Ryzhov EV. 2001. Transonic streamlining of profile at energy addition in local supersonic zone. *Proceedings of the 3-rd Workshop on magneto – plasma-aerodynamics in aerospace applications, Moscow, IVTAN*.
[51] Pav´on S, Ott P, Leyland P, Dorier J-L and Hollenstein Ch. 2009. Effects of a surface dielectric barrier discharge on transonic flows around an airfoil. *AIAA Paper, 2009-649.*